Macromolecules

ARTICLE

pubs.acs.org/Macromolecules

Strong Nanocomposite Reinforcement Effects in Polyurethane Elastomer with Low Volume Fraction of Cellulose Nanocrystals

Aihua Pei,[†] Jani-Markus Malho,[‡] Janne Ruokolainen,[‡] Qi Zhou,[*,§] and Lars A. Berglund[†,∥]

[†]Department of Fibre and Polymer Technology, Royal Institute of Technology, SE-100 44 Stockholm, Sweden

[‡]Department of Applied Physics, Aalto University, FIN-00076 Finland

[§]School of Biotechnology, Royal Institute of Technology, AlbaNova University Centre, SE-106 91 Stockholm, Sweden

[∥]Wallenberg Wood Science Center, Royal Institute of Technology, SE-100 44 Stockholm, Sweden

ABSTRACT: Polyurethane/cellulose nanocrystal nanocomposites with ultrahigh tensile strength and stain-to-failure with strongly improved modulus were prepared by adding cellulose nanocrystals (CNCs) during the preparation of prepolymer. The nanostructure of this polyurethane consisted of individualized nanocellulose crystals covalently bonded and specifically associated with the hard polyurethane (PU) microdomains as characterized by Fourier transform infrared spectroscopy and transmission electron microscopy. The storage modulus and thermal stability of the nanocomposites were significantly improved as measured by dynamic mechanical analysis. This was due to a combination of CNCs reinforcement in the soft matrix and increased effective cross-link density of the elastomer network due to CNC−PU molecular interaction. Tensile test revealed that the nanocomposites have both higher tensile strength and strain-to-failure. In particular, with only 1 wt % of cellulose nanocrystals incorporated, an 8-fold increase in tensile strength and 1.3-fold increase in strain-to-failure were achieved, respectively. Such high strength indicates that CNCs orient strongly at high strains and may also induce synergistic PU orientation effects contributing to the dramatic strength enhancement. The present elastomer nanocomposite outperforms conventional rubbery materials and polyurethane nanocomposites reinforced with microcrystalline cellulose, carbon nanotubes, or nanoclays.

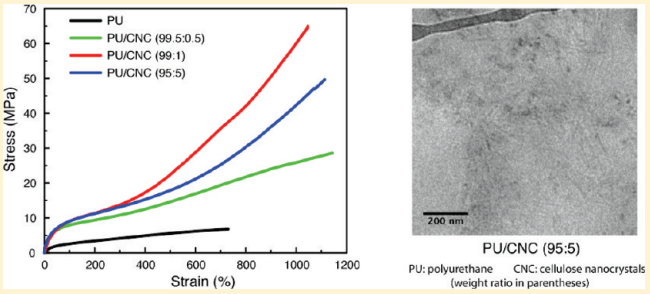

INTRODUCTION

Polymer nanocomposites reinforced with low fraction of nanoscale fillers have received steadily growing attention owing to their unique and fascinating properties that potentially rival those of the most advanced materials in nature.[1,2] Cellulose nanocrystals (CNCs) are highly crystalline rod-like nanomaterials isolated from cellulose fibers by acid hydrolysis.[3] CNCs have been incorporated into a wide range of polymer matrices as reinforcing fillers due to their appealing intrinsic properties such as nanoscale dimensions, high surface area, unique morphology, low density, high specific strength and Young's modulus, and very low coefficient of thermal expansion.[4−6] The critical challenge to achieve the transfer of the exceptional mechanical properties of crystalline cellulose to the macroscale properties of the bulk nanocomposites is the ability to obtain well-dispersed hydrophilic reinforcing nanocellulose crystals in hydrophobic polymer matrices. Yet another specific challenge is to increase the stiffness of the nanocomposites without decreasing their high extensibility. Herein, we report a novel approach to synthesize thermoplastic polyurethane with superior strength and toughness by incorporating a very low volume fraction of reactive CNCs.

Thermoplastic polyurethane is a linear block copolymer consisting of alternating soft and hard segments and often has a two-phase microstructure due to thermodynamic segmental incompatibility. The hard segment is composed of a low-molecular-weight diol or diamine (chain extender) with diisocyanate and the soft segment is composed of a high-molecular-weight polyester or polyether polyol. The soft domains are in rubbery state while the hard domains are semicrystalline or glassy at room temperature. The extensibility of the segmented polyurethane increases with soft segment content whereas the stiffness and strength increase with hard segment content.

Previously, nanometer-sized stiff and anisotropic fillers with a high aspect ratio and/or an extremely large surface area including graphite oxide nanoplatelets,[7] polyhedral oligomeric silsesquioxane,[8,9] carbon nanotubes,[10−13] and layered silicate clays[2,14−17] have been incorporated into polyurethane to enhance the mechanical performances and thermal stability. Hydrophilic layered silicate surfaces were often modified with organic surfactants to improve their compatibility with polyurethane, and thus to achieve a uniform dispersion in the nanocomposite. A decrease in disk diameter of the layered silicates was

Received: February 12, 2011
Revised: April 18, 2011
Published: May 10, 2011

associated with a pronounced increase in tensile strength of polyurethane/clay nanocomposites.[17] It is also necessary to preferentially reinforce the hard microdomains with fully exfoliated clay nanoparticles.[2]

Cellulosic nanomaterials including microfibrillated cellulose,[18] microcrystalline cellulose (MCC),[19] and CNCs[20−23] have also been used as the reinforcing filler in polyurethane. The cellulose crystal consists of stiff, close-packed extended cellulose chains with strong intermolecular forces so that Young's modulus exceeds 100 GPa in the chain direction.[24] The elastic modulus of tunicate cellulose nanocrystals was about 143 GPa, as measured by using a Raman spectroscopic technique.[25] A similar elastic modulus value was obtained for single tunicate cellulose microfibrils with a width of 20.3 nm and a thickness of 8.4 nm by a three-point bending test using an atomic force microscopy (AFM) cantilever.[26] The polyurethane nanocomposite reinforced with 16.5 wt % of cellulose nanofibrils was prepared using compression molding by stacking the cellulose fiber mats between polyurethane films, and an increase of 500% in the tensile strength was achieved.[18] Polycaprolactone-based waterborne polyurethane reinforced with CNCs isolated from flax fibers or cottonseed linter showed a significant increase in the tensile strength and Young's modulus with increasing cellulose nanocrystal content.[22,23] Similarly, the tensile modulus of polyurethane was increased from 41.16 ± 14.10 MPa to 61.99 ± 7.23 MPa and 100.2 ± 12.28 MPa with the addition of 1 and 5 wt % cellulose crystals hydrolyzed from MCC, respectively.[20,21] However, all these improvements were either realized by using large volume fractions of cellulose nanomaterial or obtained at the expense of strain-to-failure.

In our previous work,[19] high-strength and high-toughness elastomeric PU nanocomposites were prepared by dispersing more than 5 wt % MCC in the PU matrix with the addition of a trace amount of lithium chloride. In this report, we introduce nanoscale rod-like cellulose nanocrystals into the polyurethane formulation to stiffen and strengthen the material without sacrificing deformability at very low nanocrystals loadings. A much stronger reinforcing effect was observed especially at higher strain and the mechanism was investigated.

EXPERIMENTAL SECTION

Materials. Dimethylformamide (DMF, Fluka) was dried over 3 Å molecular sieves for 24 h before use. 4,4′-diphenyl-methane diisocyanate (MDI, Aldrich), Poly(tetramethylene glycol) (PTMEG, M_n = 1000, Aldrich) and 1,4-butanediol (1,4-BD) were used as received. Nanocrystals from cotton cellulose with a typical length of 100−300 nm and width of ca. 10 nm were prepared by sulfuric acid hydrolysis according to the method described previously.[27] In brief, cellulose nanocrystals (CNCs) were prepared by acid hydrolysis of cotton from 20 g Whatman No. 1 cellulose filter paper using 175 mL 64% (w/w) sulfuric acid at 45 °C for 1 h. The suspension was diluted 10-fold with deionized water, then centrifuged at 4300 rpm for 10 min to concentrate the cellulose and to remove excess aqueous acid. The resultant precipitate was rinsed, recentrifuged and dialyzed against water for 7 days. Mixed bed ion-exchange resin (Dowex Marathon MR-3 hydrogen and hydroxide form) was added to the cellulose suspension for 48 h and then removed by filtration. This procedure ensured that all ionic materials were removed except the H^+ counterions associated with the sulfate groups on the surface of the microcrystallites. The microcrystallites were further dispersed by ultrasonic treatment (Branson Sonifier Model 250 ultrasonic cell disruptor/homogenizer) at 80% output (with cooling in an ice bath) to create cellulose crystals of colloidal dimensions. To avoid the agglomeration of cellulose in polyurethane, cellulose nanocrystals were freeze-dried from dilute aqueous suspension (0.1 wt %) and redispersed in DMF at a solid content of 0.5 wt % without additives or any surface modification.[28,29]

Synthesis of Polyurethane Nanocomposite. The polyether−polyurethane prepolymer was synthesized by reacting 4,4′-diphenylmethane diisocyanate (MDI) with Poly(tetramethylene glycol) (PTMEG, M_n = 1000) in the presence of cellulose nanocrystal dispersed in DMF at 90 °C for 3 h. The solid content of the resulting prepolymer was 10 wt % in DMF. Subsequently, chain extender 1,4-butanediol was added to the prepolymer and stirred at room temperature for 3 h before casting and curing on a Teflon mold at 80 °C for 24 h to obtain a transparent film. The DMF residues in the film were removed at 80 °C under vacuum for 48 h. The amount of reactive hydroxyl group on cellulose nanocrystals was 2.8 ± 0.3 mmol/g as measured by using titration to determine the excessive isocyanate groups after mixing cellulose nanocrystals with known amount of MDI. The molar ratio of MDI to PTMEG in the prepolymer was 2:1, and total NCO/OH ratio in the polyurethane was equal to 1. Transparent polyurethane nanocomposite films containing 0.5, 1, and 5 wt % CNCs were successfully prepared by varying the amount of cellulose and 1,4-butanediol, and coded as PU/CNC-0.5, PU/CNC-1, and PU/CNC-5, respectively. Pure polyurethane films were prepared in the absence of CNCs and coded as PU.

Characterizations. Fourier transform infrared spectroscopy (FTIR) was conducted on a Perkin−Elmer Spectrum 2000 FTIR equipped with a MKII Golden Gate, single reflection attenuated total reflectance (ATR) system (Specac Ltd., London, UK). The ATR crystal was a MKII heated diamond 45° ATR top plate. X-ray diffraction (XRD) patterns were recorded by an X'Pert Pro diffractometer (model PW 3040/60) at room temperature. The CuKα radiation source was operated at 40 kV and 35 mA. Patterns were recorded by monitoring diffractions from 5° to 40°. The scan speed was 2°/min. Dynamic mechanical analysis (DMA) was carried out on a TA Instruments Q800 in tension mode. The frequency was 1 Hz and the temperature scanning rate was 3 °C/min.

Transmission electron microscopy (TEM) was carried out using Jeol JEM-3200FSC field emission microscope operating at 300 kV voltages. The images were taken in bright field mode and using zero loss energy filtering (omega type) with the slit of 20 eV. Micrographs were recorded using Gatan Ultrascan 4000 CCD camera. Specimen temperature was maintained at −187 °C during the imaging. Thin sections (~70 nm) were cut at −80 °C by Leica Ultracut UCT microtome using a 25° Diatome diamond knife. The sections were collected on 300 mesh lacey carbon grids.

The mechanical properties of the films were measured on a Universal Materials Testing Machine from Instron, U.S.A., equipped with a 500 N load cell. The tensile test was performed at 23 °C with a gauge length of 40 mm and crosshead speed of 100 mm/min. Samples were cut into rectangular strip with dimension of 80 × 5 × t mm^3, where t, the thickness, varied from 0.18 mm to 0.25 mm. For each sample, five strips were tested. Young's modulus was determined from the slope of initial low strain region. Toughness was defined as work to fracture and was calculated as the area under the stress−strain curves.

RESULTS AND DISCUSSION

Fourier transform infrared spectroscopy (FTIR) spectra of CNCs, PU, the PU/CNC nanocomposites, and a control sample, the mixture of CNCs and MDI, are shown in Figure 1. The reaction of the hydroxyl group of cellulose with MDI was proved by the detection of new bands at 1646 and 1510 cm^{-1}, corresponding to the absorption of carbonyl groups (C═O) and N−H bending deformation combined with C−N asymmetric stretching, respectively. The intensities of these absorption bands

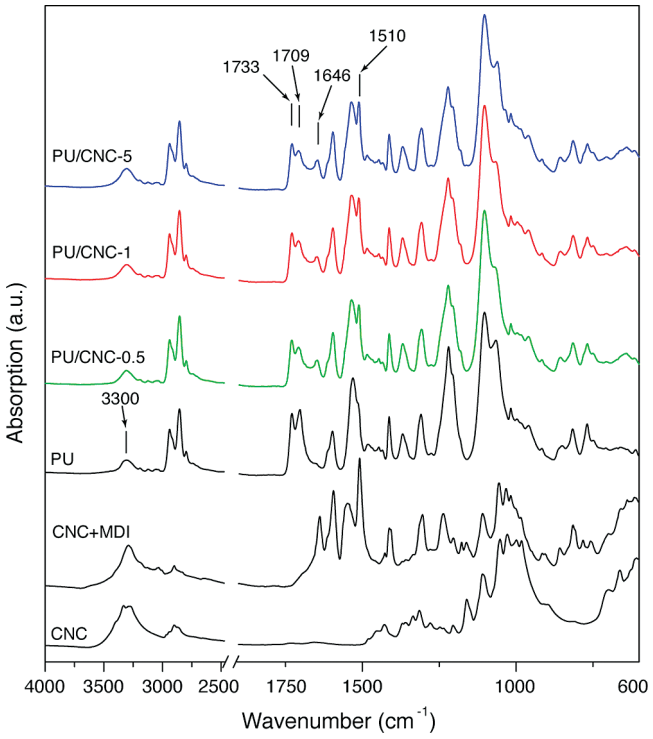

Figure 1. FTIR spectra of cellulose nanocrystals (CNCs), pure polyurethane (PU), PU/CNC nanocomposites, and a control mixture of CNCs and MDI.

increased with the increase of CNCs contents. While these bands were detected at 1709−1733 and 1540 cm^{-1} in the pure polyurethane as a result of different chemical structures and contents. Thus, the rigid rod-like cellulose nanocrystals were covalently bonded to the polyurethane molecular chains during the synthesis of prepolymer, and expected to affect the hydrogen bonding and phase separation of the segmented polyether-polyurethane. In the hard segment, the hydrogen atoms of N−H groups serve as proton donors and the urethane carbonyl groups serve as proton acceptors. If the hard and soft segments are mixed in a molecular level, the ether (C−O−C) groups can also act as proton acceptors. For all the spectra of pure polyurethane and its nanocomposites as shown in Figure 1, there is a band located at around 3300 cm^{-1} which is attributed to N−H stretching. But no bands at around 3500 cm^{-1} are detected indicating that all the N−H groups are hydrogen-bonded. The carbonyl absorption band splits into two peaks, 1709 and 1733 cm^{-1}, corresponding to hydrogen-bonded and free carbonyl groups, respectively. The carbonyl hydrogen-bonding index,[30] i.e., the intensity ratio of the hydrogen-bonded carbonyl peak to the free carbonyl peak, decreased with the increase of CNCs content since stiff nanoscale CNCs hindered the hydrogen bonding between the hard segments of polyurethane.

The phase separation of PU resulting from thermodynamic incompatibility between the soft and hard segments plays a key role in the physical properties. The influence of CNCs on the phase separation structure was also featured by the decrease of glass transition temperature (T_g) of the polyurethane. The dependence of tan δ on temperature for PU and PU/CNC nanocomposites is shown in Figure 2. The relaxation of the amorphous soft segment domains, i.e. the T_g of PU soft segments is −22.8, −35.0, −38.1, and −37.2 °C, for pure PU, PU/CNC-0.5,

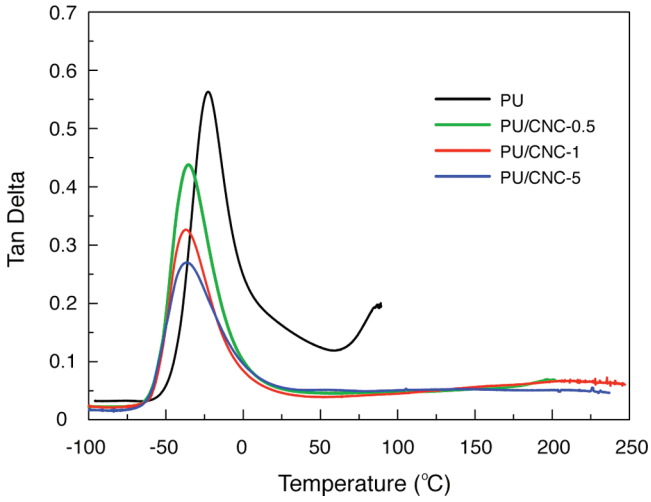

Figure 2. Damping factor tan δ of the PU and PU/CNC nanocomposites as a function of temperature.

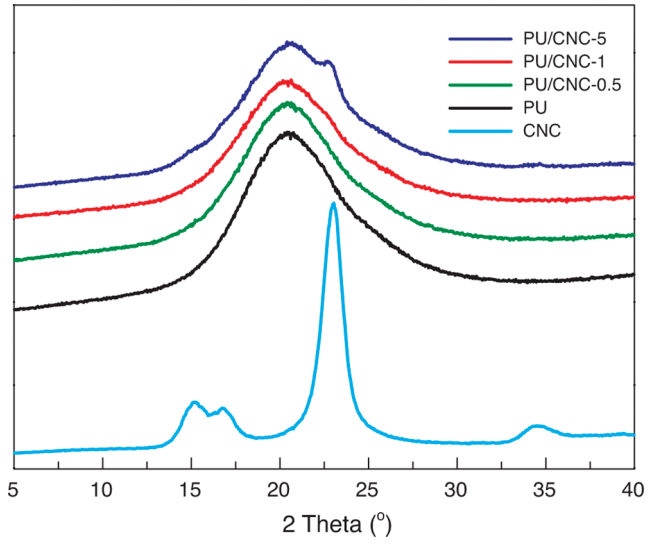

Figure 3. XRD pattern of CNCs, PU, and PU/CNC nanocomposites.

PU/CNC-1, and PU/CNC-5, respectively. The decrease of T_g for the nanocomposites is due to the fact that the CNCs are strongly associated with the hard segment of PU, resulting in lower fraction of hydrogen bonded carbonyl groups in the hard segment and an increase of the degree of freedom for the soft segment in PU. The sharpness and height of the damping peaks give information about the degree of order and the freedom of motion of the molecules in the soft domains.[31,32] The amplitude of the damping peak corresponding to the glass transition of PU decreased with increasing CNCs content while the half height width of the peak increased. This could be attributed to the greatly restricted motion of PU chains resulting from the covalent bonding and cross-linking between PU molecules and nanoscale stiff rod-like CNCs as indicated by FTIR.

The X-ray diffraction (XRD) spectra of CNCs, pure PU, and the PU/CNC nanocomposites are presented in Figure 3. The 2θ angle at 22.9° corresponds to the 200 reflection of cellulose I.[33] Because of the low content of CNCs, no obvious peaks of cellulose I were visible in PU/CNC-0.5 and PU/CNC-1, while

dx.doi.org/10.1021/ma200318k |*Macromolecules* 2011, 44, 4422–4427

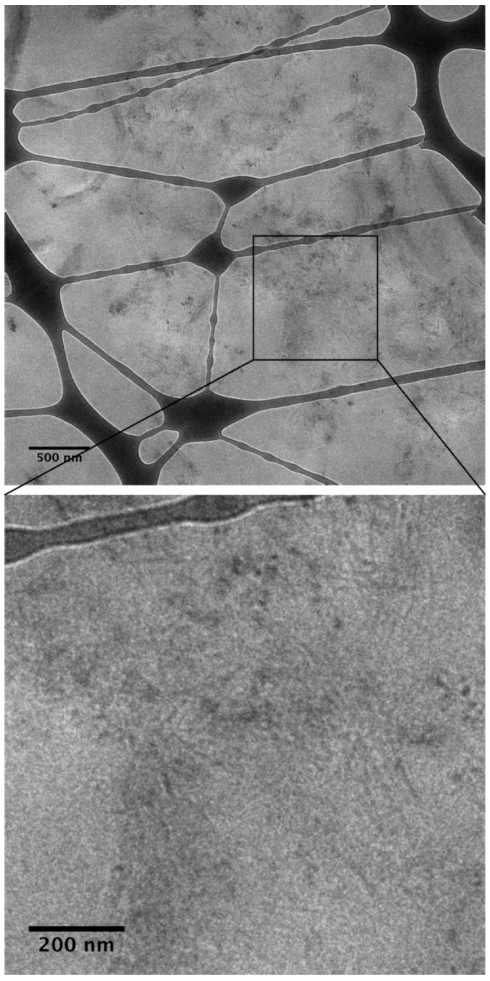

Figure 4. Transmission electron micrographs of the ultrathin cryo cross-section of polyurethane nanocomposites with 5 wt % of CNCs. Note 500 and 200 nm scale bars in lower left corners.

the peaks centered at 22.9° were clearly identified in PU/CNC-5 sample. These indicate that the original crystal structure of cellulose I was well preserved in the nanocomposites and the chemical reaction between MDI and cellulose only occurred on the surfaces of CNCs. Furthermore, CNCs were completely dispersed in the polyurethane matrix without any large agglomeration as revealed by the transmission electron microscopy (TEM). The individualized CNCs appear concentrated in certain separated domains as shown in the TEM images of the ultrathin cryo cross section of the PU nanocomposite film containing 5 wt % of CNCs (Figure 4). Such preferential distribution further indicates the incorporation of CNCs into the hard segment domains of PU that is consistent with the result of FTIR and T_g analysis.

To investigate the effect of CNCs as a reinforcing phase in the polyurethane nanocomposites, both the classical tensile tests in nonlinear range and dynamic mechanical analysis (DMA) in the linear range were performed. The dramatic impact of CNCs on the tensile and thermomechanical properties of polyurethane nanocomposites is shown in Figure 5. Pure PU showed a stress−strain curve without obvious strain hardening, while the PU nanocomposites exhibited strain hardening especially at larger elongations (Figure 5a). In particular, there is a pronounced increase in the upturn of the stress−strain curve and an increase in

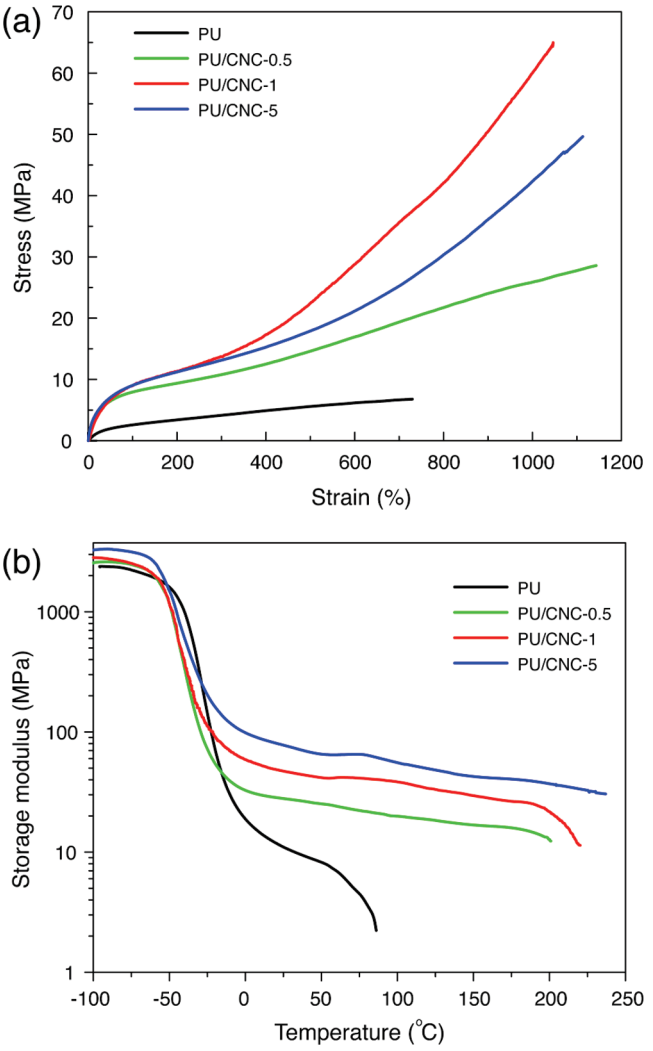

Figure 5. (a) Stress−strain curves of pure PU and PU/CNC nanocomposites. (b) Storage modulus of the PU and PU/CNC nanocomposites as a function of temperature.

Table 1. Mechanical Properties of PU and PU/CNC Nanocomposites

samples	Young's modulus (MPa)	tensile strength (MPa)	strain-to-failure (%)	work to fracture (MJ/m^3)
PU	8.2 ± 0.9	7.5 ± 1.0	751.4 ± 31.4	37.0 ± 6.2
PU/CNC-0.5	40.9 ± 3.3	26.9 ± 1.5	1087.0 ± 61.9	161.2 ± 9.3
PU/CNC-1	42.4 ± 3.0	61.5 ± 4.8	994.2 ± 75.3	317.7 ± 36.2
PU/CNC-5	44.9 ± 2.4	49.8 ± 6.6	1110.3 ± 101.1	290.2 ± 50.8

tensile strength associated with increasing strain. The introduction of CNCs as the reinforcing filler in PU led to remarkable improvement of tensile strength, strain-to-failure, Young's modulus, and work to fracture of the nanocomposites as summarized in Table 1. The tensile strength was increased from 7.5 ± 1.0 MPa for neat PU to 26.9 ± 1.5 MPa for PU/CNC-0.5, and further to 61.5 ± 4.8 MPa for PU/CNC-1 containing only 1 wt % CNCs. The Young modulus increased with CNCs contents, reaching the highest value of 44.9 ± 2.4 MPa at 5 wt % CNCs, more than

dx.doi.org/10.1021/ma200318k |*Macromolecules* 2011, 44, 4422–4427

5 times higher than that of pure PU. It is very unusual to improve the modulus while at the same time significantly improve the strength and toughness. These results indicate that the CNCs preferentially reinforce the hard microdomains rather than the soft segments of PU, avoiding the undesired stiffening of the soft domain and thus to maintain the large strain-to-failure of the polyurethane composites. In addition, the high strength indicates that CNCs orient strongly at high strains and also induce synergistic PU orientation effects contributing to the dramatic strength enhancement. To our knowledge, this is the first time such significant improvement in mechanical properties is achieved with only 1 wt % of nanoscale CNCs reinforcement of the rubbery matrix.

The dynamic mechanical analysis (DMA) allows the determination of the mechanical behavior of the materials in a broad temperature range and is strongly sensitive to the morphology and structure of the composite. A spectacular improvement in the storage modulus was achieved by introducing CNCs into the PU matrix as shown in Figure 5b. The moduli of the nanocomposites were slightly higher than that of the neat PU matrix below T_g. However, there was a significant reinforcement effect in the low modulus region above T_g. The reinforcement mechanism is both due to cellulose nanocrystal reinforcement and increased effective cross-link density of the rubber network due to PU−CNC interaction. For the neat PU reference, the modulus in Figure 5b showed a sharp decrease during the glass−rubber transition and the modulus keeps decreasing with temperature in the rubbery region due to the thermoplastic nature of the material. As for the nanocomposites, the drop in storage modulus was dramatically reduced as the PU was combined and covalently linked with CNCs. The modulus of the nanocomposites containing only 1 wt % cellulose is 400% and 1200% higher than that of pure PU at 20 and 80 °C, respectively. In addition, the introduction of CNCs also provides the nanocomposites with outstanding thermal stability up to 210−230 °C, the temperature at which cellulose starts to degrade.

The reinforcing effect of tunicate cellulose nanocrystals (also termed as whiskers) in poly(styrene-*co*-butyl acrylate) matrix were first demonstrated by Favier et al.[34] A spectacular improvement in the storage modulus was measured by DMA in the shear mode, and the increase was especially significant above the glass−rubber transition temperature. The reason for such mechanical reinforcing and thermal stability enhancement was attributed to the formation of a rigid network by the cellulose whiskers in the host polymer matrix, which was governed by the percolation mechanism. In this mechanism, the network is expected to form above the critical volume fraction at the percolation threshold, V_{Rc}, which depends on the aspect ratio (L/d) of the filler. In our case, the aspect ratio of CNCs from cotton is 10−30, leading to a V_{Rc} value of 2.3−5.0 vol %, i.e., 3.3−7.0 wt %. However, the PU/CNC nanocomposite with ultra high tensile strength and strain-to-failure was obtained from only 0.5 wt % of CNCs, which is much lower than the calculated percolation value. Thus, we can conclude that such significant modulus reinforcement effect without formation of a cellulose network is because of the introduction of a discrete reinforcement phase of nanoscale rod-like stiff CNCs, in combination with increased effective rubber cross-link density due to covalent linking of CNCs to the PU hard segments. The PU links to the CNCs through the reactive hydroxyl groups on the CNCs surface as characterized by FTIR and TEM.

The use of lignocellulosic nanomaterials derived from sustainable, annually renewable resources as a reinforcing phase in

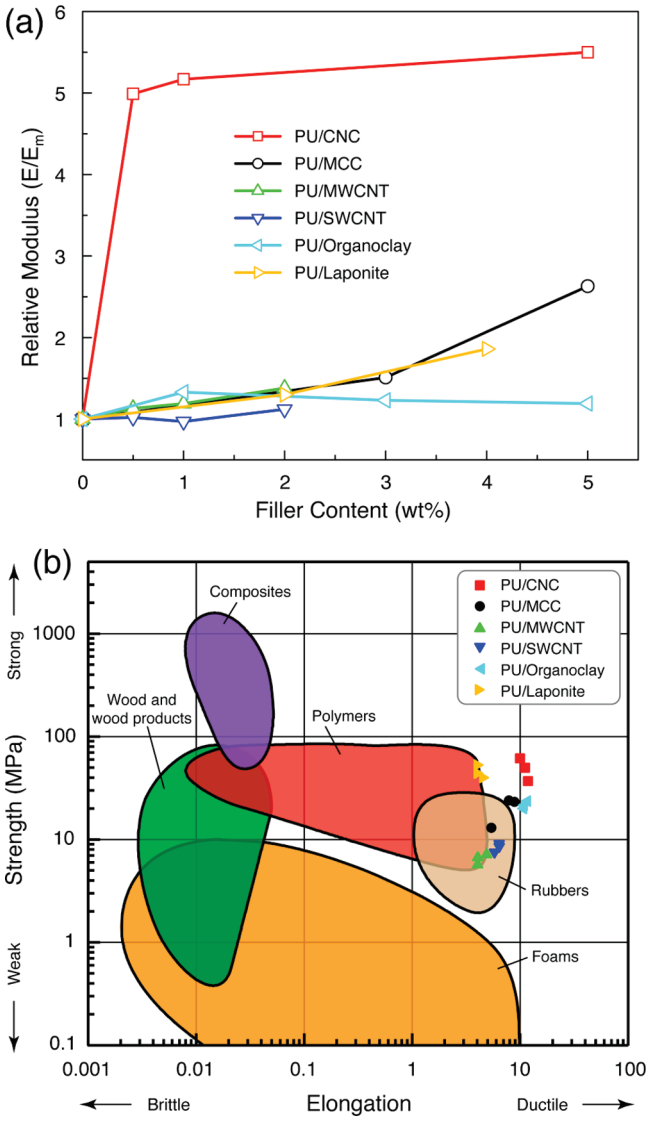

Figure 6. (a) Relative modulus (E/E_m) versus filler content for PU reinforced with CNCs (this work), MCC, MWCNT, SWCNT, organoclay, and laponite. (b) Materials selection chart adapted from Ashby and Wegst.[35] The data for PU nanocomposites were drawn based on this work and the literature.[2,12,16,19]

polymeric matrix composites has positive environmental benefits and general biological compatibility as compared to the leading candidates, e.g. carbon nanotubes and nanoclays. In addition, unlike other nanomaterials, cellulose nanocrystal manufacturing is already a sustainable and viable bulk process. Figure 6a shows the comparison of relative modulus (E/E_m) as a function of filler content for polyurethane nanocomposites reinforced with CNCs, MCC,[19] multiwalled carbon nanotubes (MWCNT) and single-walled carbon nanotubes (SWCNT),[12] organoclay,[16] and laponite.[2] E and E_m are Young's modulus values of the nanocomposites and PU matrix, respectively. The addition of very small amounts of CNCs led to the highest modulus enhancement for PU as compared to the other fillers. The efficiency of the CNCs was verified from the position of PU nanocomposites on the materials selection chart (Figure 6b). The most plausible explanation, as supported by the DMA and FTIR data is that the CNCs surface is highly functional so that the effective cross-link

density (physical and chemical) of the elastomer is increased through PU−CNC reactions. Modulus is therefore improved not only by stiff CNCs reinforcement of a soft matrix but also by effects of CNCs in the elastomer network structure. The 10 nm wide CNCs particles act as chemically highly functional cross-linking sites for the PU so that a denser elastomer network of higher modulus is obtained. The results suggest that PU nanocomposites reinforced with extremely low volume fraction of CNCs represent a good compromise between high tensile strength and high strain-to-failure, outperforming conventional rubbery materials and polyurethane nanocomposites reinforced with MCC, carbon nanotubes, or nanoclays.

■ CONCLUSIONS

In conclusion, we have demonstrated the synthesis of ultrahigh tensile strength and strain-to-failure polyurethane nanocomposites with strongly improved modulus using very low amount of biobased nanomaterial, cellulose nanocrystals, as the reinforcing filler. The individualized nanocellulose crystals were covalently bonded and specifically associated with the hard microdomains of segmented polyether−polyurethane. Such nanostructure is important to significantly stiffen and toughen the thermoplastic polyurethane without reducing its extensibility, analogous to previous observations on silicate platelet nanocomposites using laponite.[2] With the addition of only 1 wt % cellulose nanocrystals, we obtained polyurethane nanocomposite with tensile strength of 61.5 MPa, strain-to-failure of 994.2% and Young's modulus of 42.4 MPa, which surpass those of conventional rubbery materials and the polyurethane nanocomposites reinforced with low volume fraction of laponite. Our material synthetic and design strategy, i.e. creating strong nanocrystals−polyurethane interaction at the interface rather than forming a cellulose nanofibril network, has successfully solved the brittleness problem that is often rendered by adding nanocellulose crystals to polymers and elastomers. The result of this study will have a great impact on broadening the practical use and applications of cellulose nanocrystal-based polymer nanocomposite materials.

■ AUTHOR INFORMATION

Corresponding Author

*E-mail: qi@kth.se.

■ ACKNOWLEDGMENT

This work was performed at the Swedish Center for Biomimetic Fiber Engineering (Biomime; http://www.biomime.org/) funded by the Swedish Foundation for Strategic Research (SSF). For A.P. and L.A.B., part of the funding was from Wallenberg Wood Science Center. J.R. would like to acknowledge funding from the Aalto University MIDE program.

■ REFERENCES

(1) Podsiadlo, P.; Kaushik, A. K.; Arruda, E. M.; Waas, A. M.; Shim, B. S.; Xu, J. D.; Nandivada, H.; Pumplin, B. G.; Lahann, J.; Ramamoorthy, A.; Kotov, N. A. *Science* **2007**, *318*, 80–83.

(2) Liff, S. M.; Kumar, N.; McKinley, G. H. *Nat. Mater.* **2007**, *6*, 76–83.

(3) Dong, X. M.; Revol, J. F.; Gray, D. G. *Cellulose* **1998**, *5*, 19–32.

(4) Eichhorn, S. J.; Dufresne, A.; Aranguren, M.; Marcovich, N. E.; Capadona, J. R.; Rowan, S. J.; Weder, C.; Thielemans, W.; Roman, M.; Renneckar, S.; Gindl, W.; Veigel, S.; Keckes, J.; Yano, H.; Abe, K.; Nogi, M.; Nakagaito, A. N.; Mangalam, A.; Simonsen, J.; Benight, A. S.; Bismarck, A.; Berglund, L. A.; Peijs, T. *J. Mater. Sci.* **2010**, *45*, 1–33.

(5) Habibi, Y.; Lucia, L. A.; Rojas, O. J. *Chem. Rev.* **2010**, *110*, 3479–3500.

(6) Samir, M.; Alloin, F.; Dufresne, A. *Biomacromolecules* **2005**, *6*, 612–626.

(7) Cai, D. Y.; Yusoh, K.; Song, M. *Nanotechnology* **2009**, *20*, 085712.

(8) Hsiao, B. S.; White, H.; Rafailovich, M.; Mather, P. T.; Jeon, H. G.; Phillips, S.; Lichtenhan, J.; Schwab, J. *Polym. Int.* **2000**, *49*, 437–440.

(9) Liu, H.; Xu, J.; Li, Y.; Li, B.; Ma, J.; Zhang, X. *Macromol. Rapid Commun.* **2006**, *27*, 1603–1607.

(10) Sen, R.; Zhao, B.; Perea, D.; Itkis, M. E.; Hu, H.; Love, J.; Bekyarova, E.; Haddon, R. C. *Nano Lett.* **2004**, *4*, 459–464.

(11) Koerner, H.; Liu, W. D.; Alexander, M.; Mirau, P.; Dowty, H.; Vaia, R. A. *Polymer* **2005**, *46*, 4405–4420.

(12) Xia, H. S.; Song, M. *Soft Matter* **2005**, *1*, 386–394.

(13) Kwon, J.; Kim, H. *J. Polym. Sci., Part A: Polym. Chem.* **2005**, *43*, 3973–3985.

(14) Wang, Z.; Pinnavaia, T. J. *Chem. Mater.* **1998**, *10*, 3769–3771.

(15) Zilg, C.; Thomann, R.; Mulhaupt, R.; Finter, J. *Adv. Mater.* **1999**, *11*, 49–52.

(16) Tien, Y. I.; Wei, K. H. *Macromolecules* **2001**, *34*, 9045–9052.

(17) Finnigan, B.; Jack, K.; Campbell, K.; Halley, P.; Truss, R.; Casey, P.; Cookson, D.; King, S.; Martin, D. *Macromolecules* **2005**, *38*, 7386–7396.

(18) Seydibeyoglu, M. O.; Oksman, K. *Compos. Sci. Technol.* **2008**, *68*, 908–914.

(19) Wu, Q. J.; Henriksson, M.; Liu, X.; Berglund, L. A. *Biomacromolecules* **2007**, *8*, 3687–3692.

(20) Marcovich, N. E.; Auad, M. L.; Bellesi, N. E.; Nutt, S. R.; Aranguren, M. I. *J. Mater. Res.* **2006**, *21*, 870–881.

(21) Auad, M. L.; Contos, V. S.; Nutt, S.; Aranguren, M. I.; Marcovich, N. E. *Polym. Int.* **2008**, *57*, 651–659.

(22) Cao, X. D.; Dong, H.; Li, C. M. *Biomacromolecules* **2007**, *8*, 899–904.

(23) Cao, X. D.; Habibi, Y.; Lucia, L. A. *J. Mater. Chem.* **2009**, *19*, 7137–7145.

(24) Bergenstråhle, M.; Berglund, L. A.; Mazeau, K. *J. Phys. Chem. B* **2007**, *111*, 9138–9145.

(25) Sturcova, A.; Davies, G. R.; Eichhorn, S. J. *Biomacromolecules* **2005**, *6*, 1055–1061.

(26) Iwamoto, S.; Kai, W. H.; Isogai, A.; Iwata, T. *Biomacromolecules* **2009**, *10*, 2571–2576.

(27) Pei, A. H.; Zhou, Q.; Berglund, L. A. *Compos. Sci. Technol.* **2010**, *70*, 815–821.

(28) Samir, M. A. S. A.; Alloin, F.; Sanchez, J. Y.; El Kissi, N.; Dufresne, A. *Macromolecules* **2004**, *37*, 1386–1393.

(29) Viet, D.; Beck-Candanedo, S.; Gray, D. G. *Cellulose* **2007**, *14*, 109–113.

(30) Tien, Y. I.; Wei, K. H. *Polymer* **2001**, *42*, 3213–3221.

(31) Son, T. W.; Lee, D. W.; Lim, S. K. *Polym. J.* **1999**, *31*, 563–568.

(32) Tsagaropoulos, G.; Eisenberg, A. *Macromolecules* **1995**, *28*, 6067–6077.

(33) Zhou, Q.; Malm, E.; Nilsson, H.; Larsson, P. T.; Iversen, T.; Berglund, L. A.; Bulone, V. *Soft Matter* **2009**, *5*, 4124–4130.

(34) Favier, V.; Chanzy, H.; Cavaille, J. Y. *Macromolecules* **1995**, *28*, 6365–6367.

(35) Ashby, M. F.; Gibson, L. J.; Wegst, U.; Olive, R. *Proc. R. Soc. London, Ser. A* **1995**, *450*, 123–140.